Exp Brain Res (2001) 141:541–551
DOI 10.1007/s00221-001-0894-7

RESEARCH ARTICLE

C. de Waele · P.M. Baudonnière · J.C. Lepecq
P. Tran Ba Huy · P.P. Vidal

Vestibular projections in the human cortex

Received: 12 December 2000 / Accepted: 28 August 2001 / Published online: 31 October 2001

Abstract There is considerable evidence from studies on cats and monkeys that several cortical areas such as area 2v at the tip of the intraparietal sulcus, area 3av in the sulcus centralis, the parietoinsular vestibular cortex adjacent to the posterior insula (PIVC) and area 7 in the inferior parietal lobule are involved in the processing of vestibular information. Microelectrode recordings from these areas have shown that: (1) most of these cortical neurons are connected trisynaptically to the labyrinthine endorgans and (2) they receive converging vestibular, visual and somatosensory inputs. These data suggest that a multimodal cortical system is involved in postural and gaze control. In humans, recent positron emission tomography (PET) scans and functional magnetic resonance imaging (fMRI) studies have largely confirmed these data. However, because of the limited temporal resolution of these two methods, the minimum time of arrival of labyrinthine inputs from the vestibular hair cells to these cortical areas has not yet been determined. In this study, we used the evoked potential method to attempt to answer this question. Due to its excellent temporal resolution, this method is ideal for the investigation of the tri- or polysynaptic nature of the vestibulocortical pathways. Eleven volunteer patients, who underwent a vestibular neurectomy due to intractable Meniere's disease (MD) or acoustic neurinoma resection, were included in this experiment. Patients were anesthetized and the vestibular nerve was electrically stimulated. The evoked potentials were recorded by 30 subcutaneous active electrodes located on the scalp. The brain electrical source imaging (BESA) program (version 2.0, 1995) was used to calculate dipole sources. The latency period for the activation of five distinct cortical zones, including the prefrontal and/or the frontal lobe, the ipsilateral temporoparietal cortex, the anterior portion of the supplementary motor area (SMA) and the contralateral parietal cortex, was 6 ms. The short latency period recorded for each of these areas indicates that several trisynaptic pathways, passing through the vestibular nuclei and the thalamic neurons, link the primary vestibular afferents to the cortex. We suggest that all these areas, including the prefrontal area, process egomotion information and may be involved in planning motor synergies to counteract loss of equilibrium.

Keywords Vestibular evoked potentials · Vestibular cortical areas · Electrical stimulation · Vestibular nerve · Frontal cortex

C. de Waele · P.P. Vidal (✉)
Laboratoire de Neurobiologie des Réseaux Sensorimoteurs, ESA 7060, CNRS-Paris 6-Paris 7, 45 rue des Saints Pères, 75270 Paris Cedex 06, France
e-mail: cnp@ccr.jussieu.fr
Tel.: +33-1-42863397, Fax: +33-1-42863399

P.M. Baudonnière · J.C. Lepecq
Neurosciences Cognitives et Imagerie Cérébrale, UPR 640 CNRS, Groupe Hospitalier Pitié-Salpétrière, 47 Boulevard de l'Hôpital, 75651 Paris Cédex 13 Paris, France

P. Tran Ba Huy
Service ORL, Hôpital Lariboisière, 3 rue Ambroise Paré, 75010 Paris, France

Introduction

Clinical observations in patients with epilepsy (Foerster 1936; Penfield 1957; Schneider et al. 1968), cortical lesions, asymmetric caloric nystagmus (Fitzgerald and Hallpike 1942), altered perception of verticality (Brandt et al. 1994), vertigo (Brandt et al. 1995; Takeda et al. 1995) and impaired memory-guided saccades (Israël et al. 1995; Pierrot-Deseilligny et al. 1995) suggest that several cortical areas are involved in the processing of vestibular inputs in humans. Recent studies using functional imagery methods during caloric and galvanic stimulations (Friberg et al. 1985; Bottini et al. 1994, 1995; Vitte et al. 1996; Lobel et al. 1998; Bucher et al. 1998) have largely confirmed these clinical findings. They found that the posterior insula, the sulcus centralis (corresponding to area 3aV in the macaque monkey), the intraparietal sulcus (corresponding to area 2v), the supramarginal gyrus (corresponding to area 7b in the macaque

monkey), the anterior cingulate and the premotor cortex are the areas which receive vestibular afferents. These results largely corroborate previous morphological and electrophysiological data obtained in cats and monkeys (see for review Fukushima 1997; Guldin and Grüsser 1998). However, although the trisynaptic nature of the vestibulocortical pathways has been well demonstrated in these species by use of microelectrode recordings (due to the short latency of the responses following stimulation of the vestibular nerve), it is still unresolved in man. Indeed, neither positron emission tomography (PET) nor functional magnetic resonance imaging (fMRI) had sufficient temporal resolution to determine the time vestibular information arrived in each of the cortical areas or to search for a hypothetical primary vestibular cortex.

We therefore aimed to investigate whether vestibular information was simultaneously processed in parallel in each of cortical areas or whether a primary cortex distributed the afferent vestibular signals to associative areas in humans. We used the evoked potentials method because its time resolution is compatible with the 5-ms latency period of the trisynaptic pathway, which links the labyrinth sensors to the cortex in monkeys (Fukushima 1997; Guldin and Grüsser 1998). The short latency vestibular potentials (SLVPs), evoked by peroperative electrical stimulation of the vestibular nerve, were recorded in anesthetized patients by 30 subcutaneous electrodes located on the scalp. Patients included in this study either underwent vestibular neurectomy due to intractable Meniere's disease (MD) or acoustic neurinoma (AN) resection. The brain electrical source imaging (BESA) program (version 2.0, 1995; Scherg and Ebersole 1993) was used to calculate dipole sources. This allowed us to determine: (1) the cortical areas that receive the vestibular information during the first 20 ms after the stimulation and (2) the time that the synchronized vestibular volley arrives in each of these areas. Anesthesia and curarization allowed us to be sure that the evoked potentials were of vestibular and not of somesthetic origin.

Some of the results described here have already been published in abstract form (Baudonnière et al. 1996; de Waele et al. 1998).

Materials and methods

Subjects

According to the Helsinki declaration and the legislation concerning clinical studies in patients (Huriet-Serusclat law), the experimental procedures used in this study were thoroughly explained in advance, all the subjects provided informed consent and their rights were protected. The protocol was approved by the Ethics Committee of the Saint Louis Hospital (No. 94 10).

Peroperative stimulation of the vestibular nerve in anesthetized patients

Eleven patients participated in this experiment: seven patients underwent unilateral vestibular neurectomy (five left, two right) to cure medically intractable MD and four patients underwent vestibular neurinoma resection (AN). They were anesthetized with fentanyl (0.3 µg/kg) and Diprivan (2.5 mg/kg). The complete protocol included several steps described below; however, due to different constraints (availability of the patients pre- and postoperatively, surgery complexities differing in each patient), it was rarely possible to fulfill all these steps. The number in brackets indicates the number of patients who successfully underwent each stage of the protocol.

Standard clinical procedures were used for the pre- and postoperative examination of vestibular and acoustic functions. These included bithermal caloric testing, subjective vertical and horizontal measurements, pure tone and vocal audiometry, vestibular evoked myogenic potential (VEMP) testing, MRI and/or scanner investigations. Once the cranial nerves were exposed by the surgeon, the vestibular nerve was stimulated and the SLVP successfully recorded before (n=7) and after (n=6) it was sectioned at its distal end or before (n=4) and after (n=3) acoustic neurinoma resection. The vestibular nerve was also stimulated and the SLVP recorded before and after curarization (Tracrium) in patients, whose ongoing surgical treatment required this procedure (n=7; five left and two right vestibular nerve stimulations). In two patients (a left MD and a right AN), the vestibular nerve was only stimulated during curarization. Finally, as a control, the facial nerve was stimulated in one patient while recording the evoked potentials.

Stimulation protocol

Vestibular nerve stimulation during its surgical exposure in anesthetized patients

The stimulation protocol was similar for the vestibular portion of the VIIIth nerve and for the facial nerve. The current pulse generator was electrically isolated from the patients by a battery operated isolation unit. A sterile insulated bipolar stainless steel electrode, with each branch of the electrode adjusted to a distance of 1 mm apart, was used to stimulate the nerve. An operating microscope was used to place and maintain the electrode in contact with the various cranial nerves. The area of contact was 0.1 mm for each branch. Therefore, the stimulation of a given nerve refers to the physical placement of electrode tips, and cannot exclude the occurrence of current spread to other surrounding nerves such as the facial and the auditory nerves (see "Discussion").

The nerves were stimulated with 0.2-ms square pulses of current, between 0.2 and 1 mA, depending on the patient. The threshold current, which was determined for the most sensitive lead, was first determined in each subject by varying the placement of the electrodes until the minimum stimulation that could evoke an SLVP was found. The stimulation intensity was arbitrarily fixed to 3 times the threshold. Single shock stimulations were given every 85 ms (12 Hz), which allowed the evoked potentials resulting from about 500 stimulations to be recorded in the shortest possible time (approximately 40 s).

Data recording and data processing

A Nicolet SM 2000 amplifier was used to record evoked potentials through 30 active electrodes. The electrode placed on the nose was used as the reference (Fig. 1). An electrocap, which followed the 10–20 international standard, was used to standardize the placement of the electrodes. Filtered evoked potentials (band pass: 0.05–70 Hz) were stored online on the hard disk of a PC through an AD converter sampling the signal at 1 kHz.

Visualization of the records allowed contaminating artifacts to be eliminated (50, 100, 150 Hz contamination, displacement of electrodes). The mean evoked potentials were calculated for 500 stimulations for each single nerve, in a time window of within –10 to 50 ms around the stimulation.

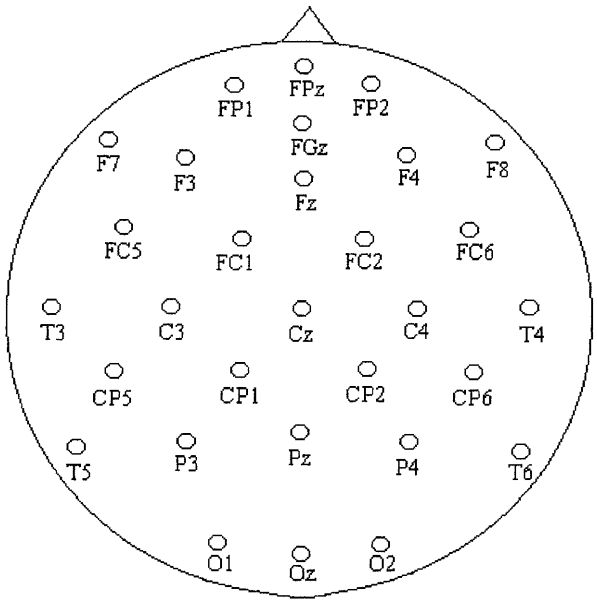

Fig. 1 Positioning of the 30 scalp electrodes

Mapping

Scalp potential maps were generated using a spherical surface spline interpolation algorithm (Perrin et al. 1989). In addition, radial scalp current density (SCD) maps were obtained by computing the second spatial derivatives of the spline functions used in potential map interpolation (Perrin et al. 1989). SCDs have the properties of being reference free and of having sharper peaks and valleys than scalp potential distributions. This facilitates interpretation in cases in which they are multiple overlapping sources.

Dipole modeling

Dipole source analysis was performed by using BESA; Scherg and Ebersole 1993; see "Materials and methods") in a four-shell spherical head model to calculate spatial-temporal models for the structures involved in the generation of the observed surface potential distributions. To obtain the dipole models, an iterative fit procedure is applied to optimize location parameters. Firstly, we attempted to use regional sources and one dipole for modeling. Residual variance and the comparison of the fitted maps with the experimental data were then used to explore the effect of progressively increasing the number of active dipoles. From a given configuration of dipoles, the resulting surface potentials were calculated and compared with the observed distribution. A numeric algorithm was used to iteratively modify the spatial parameters in order to minimize the differences (measured by *calculating the residual variance*) between the observation and the model. In our study, we added a criterion for the "goodness of fit," the *energy criterion* provided by BESA (weighted by a factor of 0.5) and a *separation criterion*. Not only the residual variance was taken into account, but also the energy of the source activity was minimized. The search for the dipoles was successful and no constraints were imposed by any of the assumptions based on electrophysiological and anatomical studies.

The Brodmann's areas corresponding to the localization of the various dipoles were calculated by use of a computer program written in our laboratory, which used the Talairach and Tournoux three-dimensional atlas of the human brain (Talairach and Tournoux 1988).

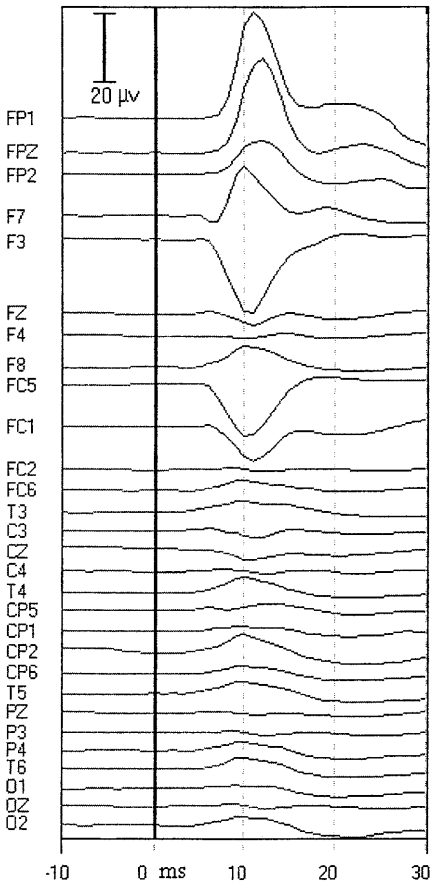

Fig. 2 SLVEPs following stimulation of the left vestibular nerve. The averaged voltage issued from the pooled data of five curarized Meniere's disease patients shows, in several electrodes, a first positive or negative deflection occurring at an average latency of 6 ms following the vestibular nerve stimulation (peak latency: 10–11 ms) and lasting about 15 ms. The major phase opposition can be observed between the ipsilateral frontal areas (FP1, FPZ, F7 vs F3, FZ, FC5, FC1). Other phase oppositions in the prefrontal, temporal, parietal and occipital areas can be noted (*ordinates* amplitude in microvolts of the evoked potentials recorded on the different scalp electrodes, *abscissa* time in milliseconds before or after the vestibular nerve stimulation, *vertical line* stimulation onset). *Scale bar* 20 µV

Results

Voltage and current source density maps following electrical stimulation of the vestibular nerve

The SLVPs were always recorded after the electrodes were placed on the vestibular portion of the VIIIth nerve, which did not induce contraction of the facial musculature. The results are presented as the mean voltage and current density maps, constructed from the pooled data of five *curarized* MD patients following stimulation of the left vestibular nerve.

Figure 2 shows the averaged records from the 30 electrodes. Following the vestibular nerve stimulation, a positive or negative deflection, lasting about 15 ms, was initially observed on several electrodes. As the sampling

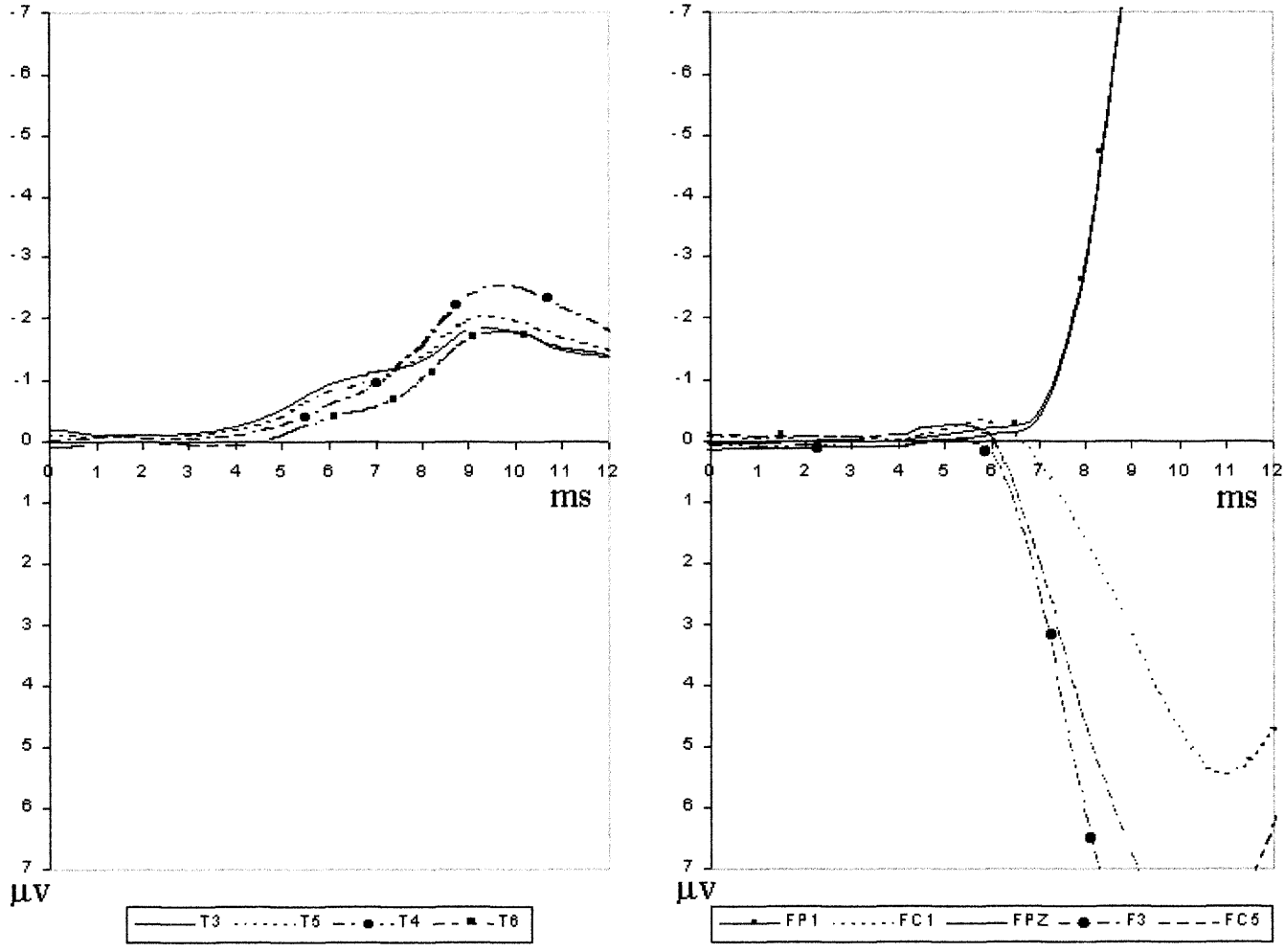

Fig. 3 Comparison of the latencies of the SLVEPs for the ipsilateral (*T3, T5*) and contralateral (*T4 and T6*), temporal (*left panel*) and frontal (*FP1, FC1, FPZ, F3 and FC5, right panel*) electrodes. Note that the mean latency to the onset of the response (2 SD above noise level) is 3.5–5 ms for the temporal electrodes and 6–7 ms for the frontal electrodes

rate used was 1 kHz, the temporal resolution of the technique was plus or minus 1 ms.

The mean latency to the onset of the response (2 SD above noise level) was statistically shorter for the temporal electrodes (3.5–5 ms, Fig. 3, left panel) than for the frontal electrodes (6–7 ms, Fig. 3, right panel). The mean latency to the peak response was close to 10 ms in all the active electrodes, in which the signal to noise ratio was sufficient to determine the latency. However, it was significantly earlier (mean: 9.5 ms; min: 9 ms; max: 10 ms, P=0.012, Student's t-test) for the temporal electrodes compared with the frontal electrodes (mean: 10.7 ms; min: 10 ms; max: 12 ms). After this initial peak, different combinations of positive and negative wave forms lasting about 25 ms were recorded. As illustrated in Fig. 2, the initial peak amplitude of the evoked potentials recorded on the frontal electrodes (FP1, F7, F3, FC5, FC1) ipsilateral to the stimulation side was always larger than those recorded on the electrodes contralateral to the stimulation side (FP2, F8, F4, FC6, FC2). Two distinct phase oppositions were observed in the ipsilateral frontal (FP1, F7 vs F3, FC5, FC1) and in the contralateral parietal (P4, T4, CP2, CP6 vs Cz, C4 areas). When the stimulation intensity was increased from 0.7 to 0.9 mA (Fig. 4), the peak amplitude of the first SLVP deflection increased on average by a factor of 2.

Voltage density maps (Fig. 5a) and current source density maps (Fig. 5b) were constructed from the mean records of the five curarized MD patients shown in Fig. 2. These two types of maps are presented using three different orientations: front view on the top row, left view on the middle and rear view on the bottom row. The current density maps (Fig. 5b) show four distinct activated zones: a prominent activation throughout the prefrontal and/or frontal lobe ipsilateral to the side of the vestibular nerve stimulation (Fig. 5b front and left view), and three other areas of activation approximately corresponding to the ipsilateral temporoparietal cortex (Fig. 5b, left and rear view), the contralateral premotor cortex (Fig. 5b, rear view) and the contralateral parietal cortex (Fig. 5a, rear view). Of course, this description is just an approximate view, a first guide for a more precise modelization with the BESA program.

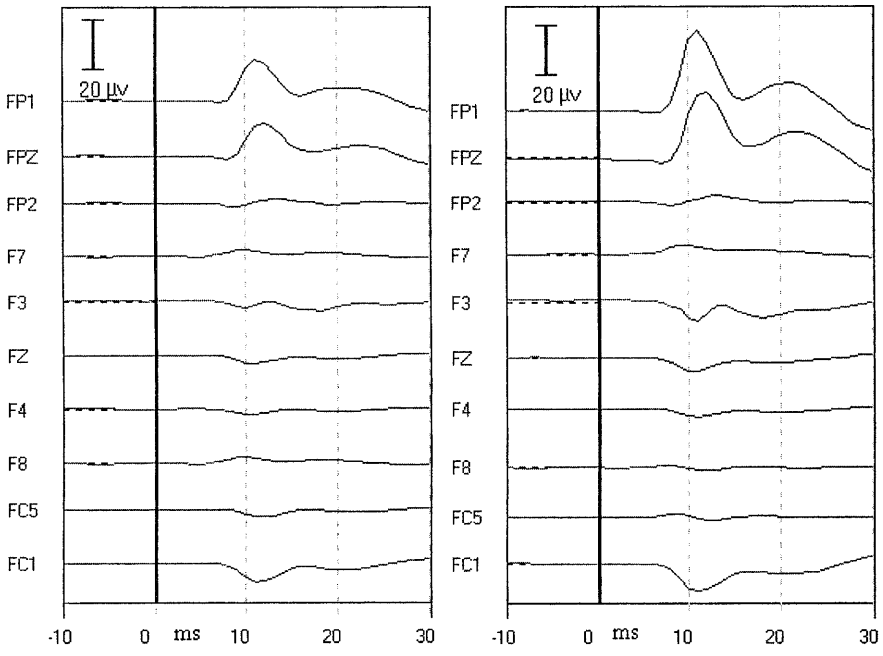

Fig. 4 Comparison at the same scale of the amplitudes of the responses recorded for two different intensities of stimulation (0.7 mA *on the left panel* and 0.9 mA *on the right panel*). Note that the amplitude of the SLVEPs increases with increasing intensities of electrical stimulation. *Scale bar* 20 µV

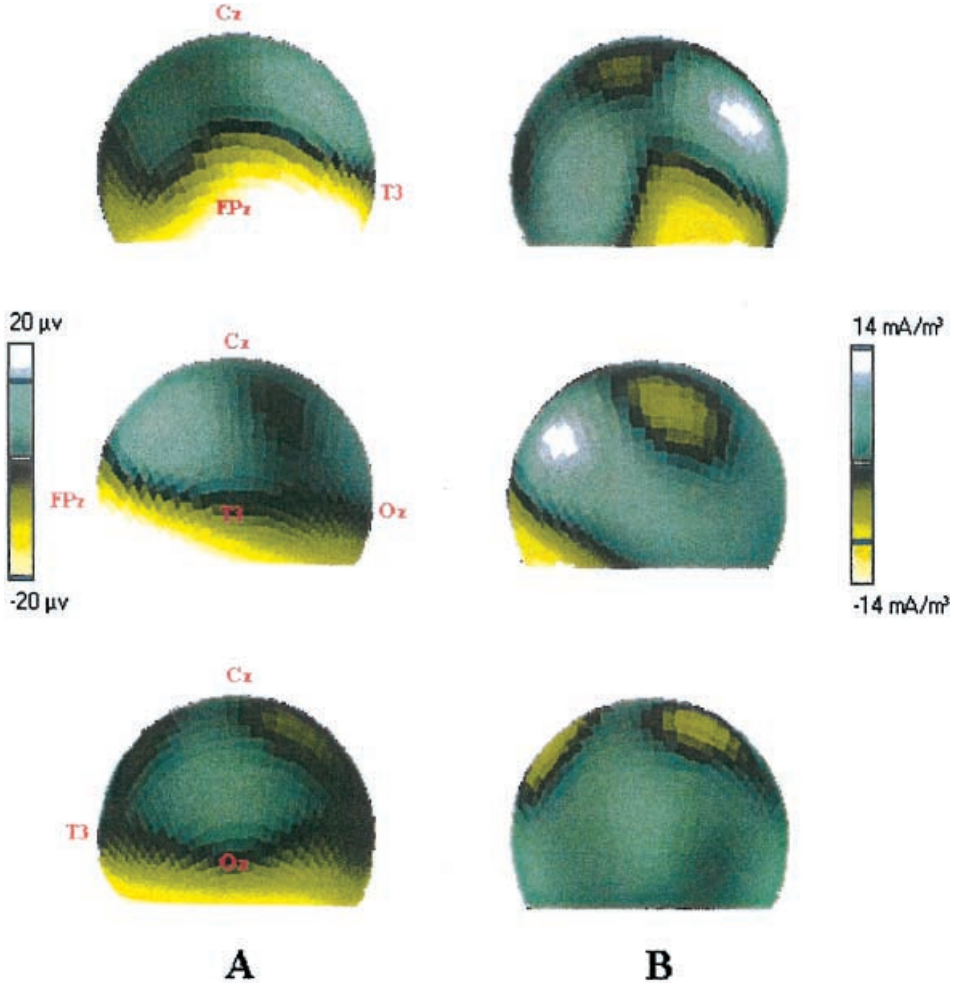

Fig. 5 Voltage **(a)** and current source density **(b)** maps issued from the pooled data of five Meniere's disease patients. These two types of maps are presented using three different orientations: front view *on the top*, left view *on the middle* and rear view *on the bottom*. The current density maps show four different activated zones: a prominent activation involving the ipsilateral prefrontal and frontal lobes (**b**, front and left view) and three other areas of activation roughly corresponding to the ipsilateral temporo-parietal area (**b**, left and rear view), the contralateral premotor area (**b**, rear view) and the contralateral parietal cortex (**a**, rear view)

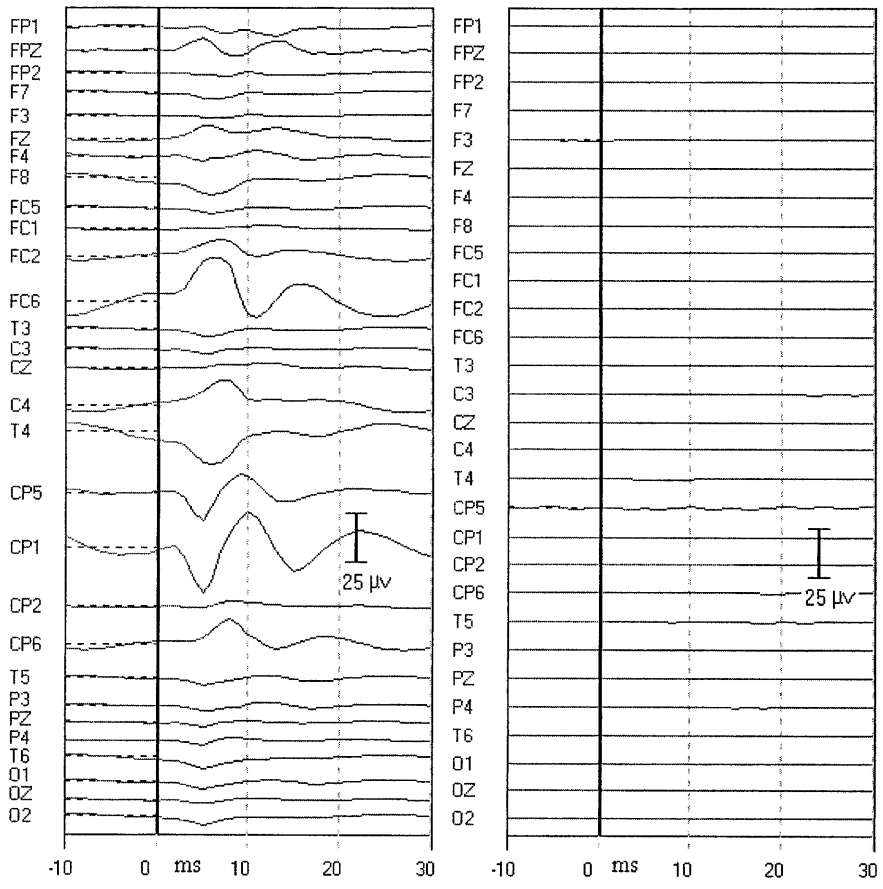

Fig. 6 Short latency evoked potentials following stimulation of the facial nerve before (*left side*) and after curarization (*right side*). The evoked potentials were larger in amplitude than those obtained following stimulation of the vestibular nerve. In addition, they completely disappeared after curarization. *Scale bar* 25 µV

The topography of the activated areas between the end of the first peak (15 ms after the onset of the stimulation) and the return of the signal to the baseline, 30 ms later, was a simple reversal of the electric fields recorded during the first 15 ms. No new cortical areas appeared to be invaded by the afferent vestibular volley, after the first 15 ms following the electrical shock in the anesthetized subject.

The data were also analyzed for each individual patient. The onset and peak latency of the SLVP were comparable for all the seven MD subjects studied in detail. Similarly, there was no consistent difference with the overall pattern of activation described by pooling the data from the five patients who were left stimulated. There was mirror symmetry in the activated areas in patients whose left or right sides were stimulated (not illustrated). In contrast to their homogeneous topography, the SLVP amplitudes differed from one patient to another and sometimes from one series of stimulations to another in the same subject. This may have been due to the manual positioning of the stimulating electrodes or to the variable state of the operating field. The only consistent change was a decrease in the amplitude of the evoked potentials with curarization.

Control stimulations

As a first control, the vestibular portion of the VIIIth nerve was electrically stimulated before and after its section in three curarized patients. In all cases, sectioning the vestibular nerve led to a threefold decrease in the short latency vestibular evoked potential (SLVEP) amplitude, when the distal stump of the vestibular portion of the VIIIth nerve was stimulated after the section. In all these cases, the lack of impairment of the auditory function after the operation shows that the acoustic portion of the VIIIth nerve was preserved after the section.

To evaluate the current spread to the facial nerve, this nerve was electrically stimulated in one patient before and after curarization. The latency and topography of the evoked potentials were completely different from the SLVP evoked by the VIIIth nerve stimulation (Fig. 6, left). Curarization abolished these evoked potentials in this patient, which indicates their somesthesic origin and confirms the efficacy of the curarization procedure used (Fig. 6, right).

Electrical source analysis of grand and individual averages after the electrical stimulation of the vestibular portion of the VIIIth nerve in curarized patients

Pooled data from the five curarized MD patients who were stimulated on the left side (grand mean) were used

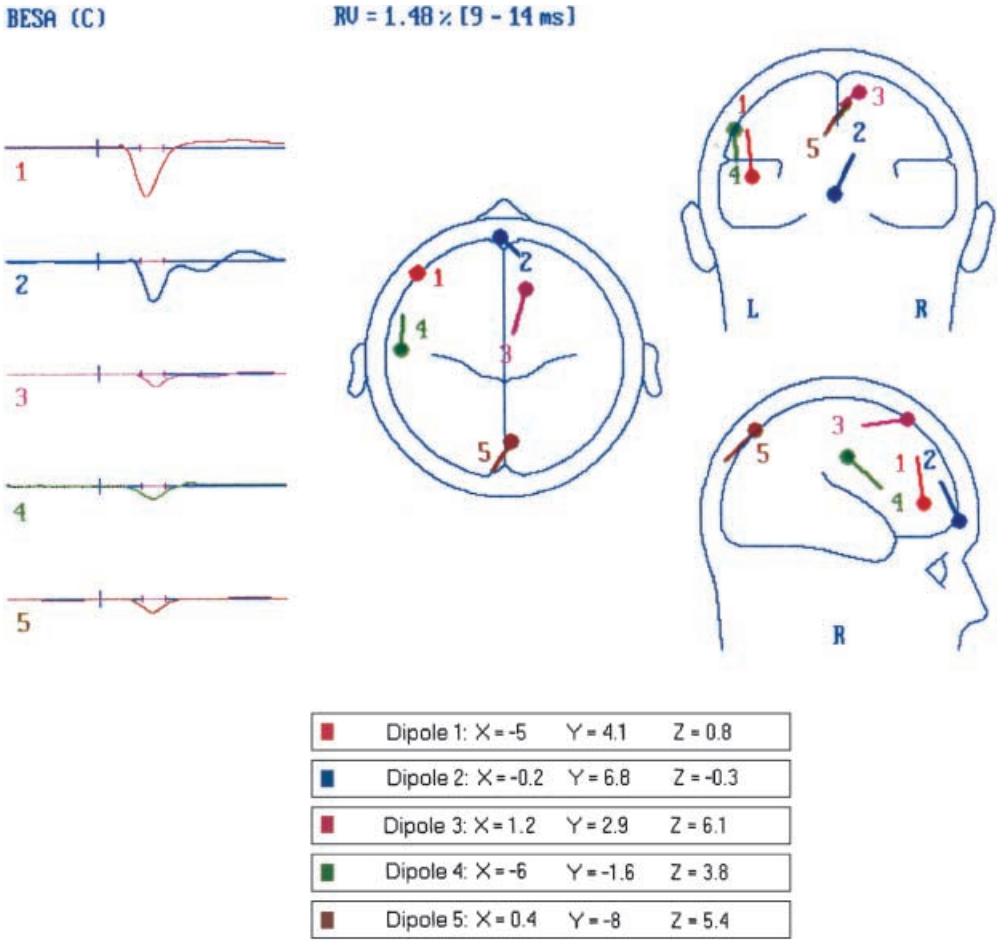

Fig. 7 Electrical source dipole analysis on the grand average. Dipole 1 is localized at the limit of the ipsilateral frontal and prefrontal lobes; dipole 2 on the transverse frontopolar and/or frontomarginal gyrus of the prefrontal lobe, close to the midline; dipole 3 on the contralateral anterior portion of the SMA (around the SEF); dipole 4 on the ipsilateral temporoparietal area; and dipole 5 on the contralateral superior occipital gyrus, although close to the midline. The *X*, *Y* and *Z* values correspond to coordinates in the Talairach and Tournoux stereotaxic atlas (1988)

to develop the model. The model was then applied to the seven individual patients.

Dipole source analysis was performed by using BESA (Scherg and Ebersole 1993). Fit criteria selected were: 20% for energy, 30% for variance minimum and 30% for separation. Firstly, we attempted to use regional sources and one dipole for modeling. Residual variance and the comparison of the fitted maps with the experimental data were then used to explore the effect of progressively increasing the number of active dipoles (see "Materials and methods" section). The best resulting model consisted of five regional sources, with a residual variance of 0.41% within a 9- and 14-ms time window. Then, we fixed the locations of sources and computed the orientation of each of the five dipoles: the residual variance was then 1.48%. Dipoles 1 and 2 were up to 5 times more active than dipoles 3, 4 and 5. Each dipole was then arbitrarily placed one by one in various localizations to test whether the BESA program could find other minima. All these attempts caused the dipoles to return to their initial position.

Secondly, electrical source dipole analysis of the grand average was mapped onto the Talairach and Tournoux stereotaxic atlas (1988). Dipoles were classified according to their decreasing amplitude (Fig. 7, left vestibular nerve stimulation) and were located as follows:

Dipole 1 was at the limit of the ipsilateral frontal and prefrontal lobe on the ipsilateral superior frontal gyrus.

Dipole 2 was on the transverse frontopolar and/or frontomarginal gyrus of the prefrontal lobe, close to the midline.

Dipole 3 was on the contralateral anterior portion of the supplementary motor area (SMA) (around the supplementary eye field, SEF).

Dipole 4 was on the ipsilateral temporoparietal area, on the precentral gyrus.

Dipole 5 was on the contralateral superior occipital gyrus.

We also applied the model constructed from the grand mean to each of the five patients whose left side was stimulated and then in the two patients whose right side was stimulated. In these right-stimulated patients, we mirror this model. Clearly, the locations of the dipoles were similar in different patients and to the grand mean. Similarly, the individual residual variances were very low, although slightly higher than for the grand mean (residual variance less than 2%).

Finally, current source spline maps obtained from the raw data were compared with current source spline maps modeled from the dipoles determined by the BESA program. The upper row (Fig. 8) shows the maps obtained from averaged raw data 9, 10, 11, 12 and 13 ms after the

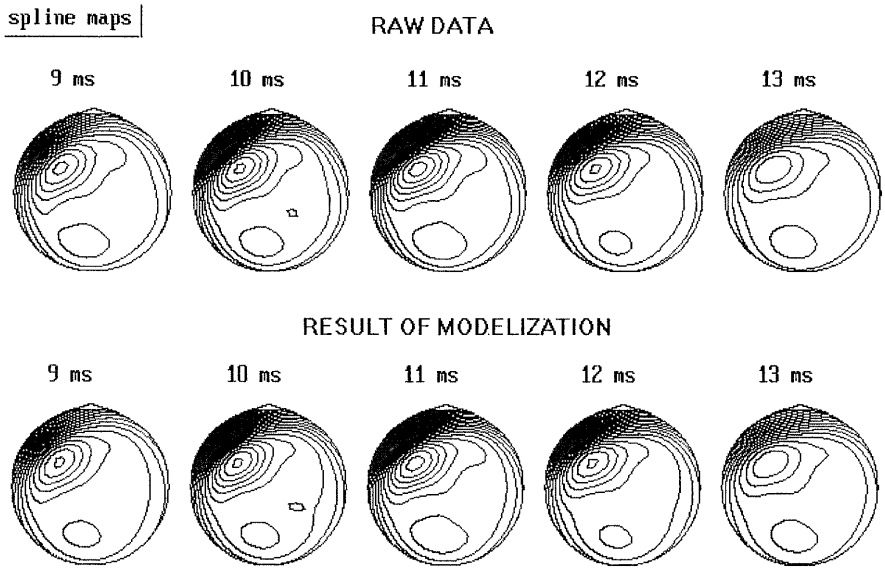

Fig. 8 Current source spline maps obtained from averaged raw (*upper part*) and modelized (*lower part*) data at 9, 10, 11, 12 and 13 ms following the vestibular nerve stimulation

vestibular nerve was stimulated, whereas the lower row (Fig. 8) corresponds to the maps resulting from the modeling at the same times.

Discussion

Our results showed that five distinct cortical zones were activated within 6 ms following vestibular nerve stimulation. These data strongly suggest that vestibular information is simultaneously processed in parallel in different cortical areas and that a primary cortex is probably not involved in the distribution of the afferent vestibular signals over associative areas.

Current spread to adjacent structures and other sources of artifacts

Current spread to the facial and acoustic nerve

Current spread to the facial nerve is probably not a source of artifact for three reasons:

1. The SLVPs were always recorded following placement of the electrodes on the VIIIth nerve, which did not cause the facial muscles to contract.
2. Direct stimulation of the facial nerve evoked potentials, which were 4 times larger than the SLVP and had a very different topography.
3. Although smaller in amplitude, the SLVP had a similar topography in curarized and non-curarized patients.

Current spread to the acoustic nerve may have been another source of artifact. Nevertheless, three criteria helped to differentiate the auditory from the vestibular areas of projections. The middle latency auditory evoked potentials (MLAEPs), which correspond to auditory activation in the subcortical nuclei or in the primary auditory cortical areas, have a minimum latency of 17 ms at the Heschl gyri (Celesia et al. 1976; Deiber et al. 1988; Fischer et al. 1994; Liegeois-Chauvel et al. 1994). This contrasts with the 6-ms latency of the SLEVP in the anesthetized patients. In addition, neither the shape nor the SLVEP topography matched the well-known MLAEP topography (see reference above). Finally, in three curarized patients, sectioning the vestibular nerve caused a threefold decrease in the amplitude of the SLVP when the distal stump of the vestibular nerve was stimulated. The remaining signal could be attributed to current spread to the proximal end of the sectioned nerve.

Eye movements

Electrical stimulation of the vestibular nerve may have evoked minute eye movements (not monitored here), which could be a potential source of artifact for the frontal and prefrontal electrodes. We do not believe that this is the case in the anesthetized subject for the following reasons:

1. Curarization did not modify the topography or the latency of the prefrontal SLVEP. This is a good control because curarization most probably suppressed the eye movements as it suppressed the facial muscle twitches induced by direct stimulation of the facial nerve.
2. The 6-ms SLVP latency period appeared to be too short to be induced by eye movements.
3. The prefrontal SLVPs were restricted to the ipsilateral side of the stimulation whereas eye movement artifacts would be expected to be bilateral.
4. The scalp electrodes such as F3, but also FC1 or FC5 which respond to the frontal SLVP, were too posterior to be contaminated by oculomotor signals and in phase opposition with other frontal electrodes.

Subcortical activations

Finally, it could be argued that the SLVEPs partly originated from dipoles located in the subcortex. The fact that current source density maps were more sharply defined than the voltage source density maps eliminated that possibility.

Parallel trisynaptic pathways mediating the SLVEPs

The earlier SLVEPs detected between 3 and 4 ms by the ipsilateral electrodes located at the lower part of the temporal lobe (T3, T5, see Fig. 3) most probably correspond to the depolarization of the second-order vestibular neurons. First, this value is similar to the temporal SLEVP latencies recorded in humans during head angular (Elidan et al. 1991) and linear (Knox et al. 1993) accelerations and following peroperative stimulations of the vestibular nerve (Häusler and Kasper 1991), which are believed to be generated at the vestibular nuclei level. Second, the region we stimulated was approximately 1.6 cm from the brainstem and 2.5 cm from the vestibular nuclei (Lang 1981). If the largest first-order vestibular neurons conducted at approximately 100 m/s (Colebatch et al. 1994), the minimum conduction time between the locus of stimulation and the vestibular nuclei would be approximately 2.5 ms. Synaptic delay lasts approximately 0.5 ms. Therefore, the onset of the depolarization of the second-order vestibular neurons probably began at 3 ms, which is consistent with previous estimations in human studies (Häusler and Kasper 1991; Elidan et al. 1991; Knox et al. 1993). For the two contralateral electrodes (T4, T6; Fig. 3), the latency appears to be larger. This could be due to the activation of the contralateral vestibular nuclei through excitatory commissural fibers. However, due to the signal to noise ratio of the method, it is extremely difficult to draw any conclusions.

The second relay of the vestibular information is thalamic. Data (see Faugier-Grimaud and Ventre 1989 for a summary) suggest that the nucleus ventralis posterior inferior, the magnocellular division of the medial geniculate body and the intralaminar nuclei are relays for the vestibular afferences. Data from monkeys (see Hawrylyshyn et al. 1978) showed that a minimum 2.5-ms delay occurs between the thalamic and the cortical neuron discharge (5 ms from the vestibular nerve to the cortex minus 2.5 ms from the vestibular nerve to the thalamus). Hence, the minimum latency compatible with a trisynaptic pathway linking the vestibular nerve to the vestibular nuclei (2 ms), the vestibular nuclei to the thalamus (1.5 ms) and the thalamus to the cortex (2.5 ms) should be approximately 6 ms, which is consistent with our results. As five distinct cortical areas were simultaneously activated by the electrical stimulation of the vestibular nerve, a primary vestibular cortex probably does not process vestibular information before distributing them to associative areas. Trisynaptic parallel processing in distinct cortical areas is more likely.

Comparison with previously described topography of the vestibular cortical projections

Apart from the early activation, corresponding probably to the vestibular nuclei depolarization (see above), a first cortical projection encompasses mostly the temporoparietal area, ipsilateral to the vestibular nerve stimulation. This area was previously described in human studies by the use of PET scans and fMRI studies (Bottini et al. 1994, 1995; Vitte et al. 1996; Lobel et al. 1998; de Waele et al. 1998; Bucher et al. 1998). This area is probably homologous to all or some of the areas defined as an "inner circle" of vestibular cortical representations in monkeys, including areas PIVC (parietoinsular vestibular cortex), and 3a and 2V (Akbarian et al. 1993; Grüsser et al. 1990a, 1990b; Guldin et al. 1992).

The second projection area was the contralateral anterior portion of the SMA, which probably includes the SEF. This area was also activated in the studies mentioned above. The SEF is involved in spatiotopic memory-guided saccades following vestibular input (Pierrot-Deseilligny et al. 1993; Gaymard et al. 1990). More generally, the SEF may be involved in generating motor programs to coordinate gaze shifts and body movements (see Pierrot-Deseilligny et al. 1995 for a review).

A third and fourth area of projection were located on the prefrontal lobe ipsilateral to the vestibular nerve stimulation, close to the midline and laterally at the limit of the prefrontal and frontal lobe, on the superior frontal gyrus. These results are difficult to interpret due to the absence of corroborating electrophysiological recordings. However, convergent evidence from previous studies suggests that these regions may process egomotion-related information. A PET study (Bottini et al. 1994) indicated a huge deactivation of the prefrontal lobe following caloric stimulation. An fMRI study during optokinetic stimulation (Bucher et al. 1997) demonstrated an activation of the prefrontal lobe. More recently, the frontal premotor regions were bilaterally activated during galvanic vestibular stimulation using fMRI (Lobel et al. 1998). Our recent PET study using high level click stimuli showed an activation of the frontoinsular gyrus (de Waele et al. 1998). Saccular afferents were recently shown to respond to loud clicks (Colebatch et al. 1994; de Waele et al. 1999). In addition, patients with circumscribed lesions of the frontal and prefrontal lobes have impairments of: (1) perception of verticality (Teuber and Mishkin 1954), (2) memory-guided saccades based on vestibular inputs (Pierrot-Deseilligny et al. 1991, 1993; Israël et al. 1995) and (3) postural reactions during voluntary movements and respiration (Gurfinkel and Elner 1988). Finally, electrical shock of the prefrontal cortex triggers the illusion of motion (Munari et al. 1995; Rasmussen 1983). Therefore, we propose a working hypothesis in which this prefrontal area: (1) may process egomotion information and (2) may be involved in planning motor synergies to counteract loss of equilibrium whether they are predicted (voluntary movements) or unpredicted (reactions to falls).

Conclusion

We showed that several cortical areas are linked to the vestibular nerve by trisynaptic pathways in humans. This finding does not support the notion of a primary vestibular cortex, which would redistribute the afferent vestibular signals over other associative areas. Parallel processing of the vestibular information from the vestibular nerve to these five cortical areas appears to be more likely. The prefrontal cortex seems to be involved in the processing of vestibular information.

Acknowledgements We thank B. Renault, our colleagues from the Laboratory of Neurosciences Cognitives et Imagerie Cérébrale and Franck Zamith from the ENT Department of the Lariboisière Hospital for their advice and help. The studies were supported by the Contrat de Recherche Clinique AP No 93 1807.

References

Akbarian S, Grüsser OJ, Guldin W (1993) Corticofugal projections to the vestibular nuclei in squirrel monkeys: further evidence of multiple cortical vestibular fields. J Comp Neurol 332:89–104

Baudonnière PM, de Waele C, Tran Ba Huy P, Vidal PP (1996) Vestibular evoked responses before and immediately after unilateral vestibular neurectomy in human. In: Collard M, Jeannerod M, Christen Y (eds) The vestibular cortex. Irvinn, Strasbourg, pp 89–102

Bottini G, Sterzi R, Paulesu E, Vallar G, Cappa SF, Erminio F, Passingham RE, Frith CD, Frackowiak RSJ (1994) Identification of the central vestibular projections in man: a positron emission tomography activation study. Exp Brain Res 99:164–169

Bottini G, Paulesu E, Sterzi R, Warburton E, Wise RJS, Vallar G, Frackowiak RSJ, Frith CD (1995) Modulation of conscious experience by peripheral sensory stimuli. Nature 376:778–781

Brandt T, Dieterich MA, Danek A (1994) Vestibular cortex lesions affect the perception of verticality. Ann Neurol 35:403–412

Brandt T, Betzet K, Yousry T, Dieterich MA, Schulze S (1995) Rotational vertigo in embolic stroke of the vestibular and auditory cortices. Neurology 45:42–44

Bucher SF, Dieterich MA, Klaus C, Seelos MD, Brandt T (1997) Sensorimotor cerebral activation during optokinetic nystagmus. A functional MRI study. Neurology 49:1370–1377

Bucher SF, Dieterich M, Wiesmann M, Weiss A, Zink R, Yousry TA, Brandt T (1998) Cerebral functional magnetic resonance imaging of vestibular, auditory and nociceptive areas during galvanic stimulation. Ann Neurol 44:120–125

Celesia GG (1976) Organization of auditory cortical areas in man. Brain 99:403–414

Colebatch JG, Halmagyi GM, Skuse MF (1994) Myogenic potentials generated by a click-evoked vestibulocollic reflex. J Neurol Neurosurg Psychiatry 57:190–197

Deiber MP, Ibanez V, Fischer C, Perrin F, Mauguière F (1988) Sequential mapping favors the hypothesis of distinct generators for Na and Pa middle latency auditory evoked potentials. Electroencephalogr Clin Neurophysiol 71:187–197

de Waele C, Baudonnière PM, Ballester M, Belin P, Samson Y, Tran Ba Huy P, Vidal PP (1998) Localization of cortical otolithic vestibular projections in humans: an evoked potentials and PET scan study. In: Abstract book of the forum meeting of European neuroscience, Berlin. Eur J Neurosci 10 Suppl 10: abstract 151.05, pp 361

de Waele C, Tran Ba Huy P, Diard JP, Freyss G, Vidal PP (1999) Saccular dysfunction in Meniere's disease. Am J Otol 20:223–232

Elidan J, Leibner E, Freeman S, Sela M, Nitzan M, Sohmer H (1991) Short and middle latency vestibular evoked responses to acceleration in man. Electroencephalogr Clin Neurophysiol 80:140–145

Faugier-Grimaud S, Ventre J (1989) Anatomic connections of inferior parietal cortex (Ba7) with subcortical structures related to vestibulo-ocular function in monkey (*Macaca fascicularis*). J Comp Neurol 280:1–14

Fischer C, Bognar L, Turjman F, Villanyi E, Lapras C (1994) Auditory early and middle-latency evoked potentials in patients with quadrigeminal plate tumors. Neurosurgery 35:45–51

Fitzgerald G, Hallpike CS (1942) Studies in human vestibular function: I. Observation on the directional preponderance (Nystagmusbereitschaft) of caloric nystagmus resulting from cerebral lesions. Brain 65:115–137

Foerster O (1936) Sensible korticale Felder. In: Bumke O, Foerster O (eds) Handbuch der Neurologie, vol VI. Springer-Verlag, Berlin, pp 358–449

Friberg L, Olsen TS, Roland PE, Paulson OB, Lassen NA (1985) Focal increase of blood flow in the cerebral cortex of man during vestibular stimulation. Brain 108:609–623

Fukushima K (1997) Cortico-vestibular interactions: anatomy, electrophysiology, and functional considerations. Exp Brain Res 117:1–16

Gaymard B, Pierrot-Deseilligny C, Rivaud S (1990) Impairment of sequences of memory-guided saccades after supplementary motor Ba lesions. Ann Neurol 28:622–626

Grüsser OJ, Pause M, Schreiter U (1990a) Localization and responses of neurones in the parieto-insular vestibular cortex of awake monkeys. J Physiol (Lond) 430:537–557

Grüsser OJ, Pause M, Schreiter U (1990b) Vestibular neurons in the parieto-insular cortex of monkeys (*Macaca fascicularis*): visual and neck receptor responses. J Physiol (Lond) 430:559–583

Guldin WO, Grüsser OJ (1998) Is there a vestibular cortex? Trends Neurosci 21:254–259

Guldin WO, Akbarian S, Grüsser OJ (1992) Cortico-cortical connections and cytoarchitectonics of the primate vestibular cortex: a study in squirrel monkeys (*Saimiri sciureus*). J Comp Neurol 401:326–375

Gurfinkel VS, Elner AM (1988) Contribution of the frontal lobe secondary motor Bato organization of postural components in human voluntary movement. Neirofiziologiya 20:7–15

Häusler R, Kasper A (1991) Triple monitoring électrophysiologique per-operatoire de la neurectomie vestibulaire. Ann Otol Rhinol Laryngol 108:319–323

Hawrylyshyn PA, Rubin AM, Tasker RR, Organ LW, Fredrickson JM (1978) Vestibulothalamic projections in man – a sixth primary sensory pathway. J Neurophysiol 41:394–401

Israël I, Rivaud S, Gaymard B, Berthoz A, Pierrot-Deseilligny C (1995) Cortical control of vestibular-guided saccades in man. Brain 118:1169–1183

Knox GW, Isaacs J, Woodard D, Johnson L, Jordan D (1993) Short latency vestibular evoked potentials. Otolaryngol Head Neck Surg 108:265–269

Lang J (1981) Facial and vestibulocochlear nerve, topographic anatomy and variations. In: Samii APJ (ed) Springer-Verlag, New York, pp 363–377

Liegeois-Chauvel C, Mussolino A, Badier JM, Marquis P, Chauvel P (1994) Evoked potentials recorded from the auditory cortex in man: evaluation and topography of the medial latency components. Electroencephalogr Clin Neurophysiol 92:204–214

Lobel E, Kleine JF, Le Bihan D, Leroy Willig A, Berthoz A (1998) Functional MRI of galvanic vestibular stimulation. J Neurophysiol 80:2699–2709

Munari C, Berta E, Minotti L, Di Leo M, Hoffmann D, Tassi L, Kahane P, Lo Russo G, Francione S (1995) Contribution to the identification of "vestibular" cortex in man: a stereo EEG study. In: Collard M, Jeannerod M, Christen Y (eds) Le cortex vestibulaire. Irvinn, Strasbourg, pp 48–63

Penfield W (1957) Vestibular sensation and the cerebral cortex. Ann Otol Rhinol Laryngol 66:691–698

Perrin F, Pernier J, Bertrand O, Echallier JF (1989) Spherical splines for scalp potential and current density mapping. Electroencephalogr Clin Neurophysiol 72:184–187

Pierrot-Deseilligny C, Rivaud S, Gaymard B, Agid Y (1991) Cortical control of memory-guided saccades in man. Exp Brain Res 83:606–617

Pierrot-Deseilligny C, Israël I, Berthoz A, Rivaud S, Gaymard B (1993) Role of the different frontal lobe areas in the control of the horizontal component of memory-guided saccades in man. Exp Brain Res 95:166–171

Pierrot-Deseilligny C, Rivaud S, Gaymard B, Vermersch A (1995) Cortical control of saccades. Ann Neurol 37:557–567

Rasmussen T (1983) Characteristic of a pure culture of frontal lobe epilepsy. Epilepsia 24:482–493

Scherg M, Ebersole JS (1993) Models of brain sources. Brain Topogr 5:419–423

Schneider RC, Calhoun HD, Crosby EC (1968) Vertigo and rotational movement in cortical and subcortical lesions. J Neurol Sci 6:493–516

Takeda N, Tanaka-Tsuji M, Sawada T, Koizuka I, Kubo T (1995) Clinical investigation of the vestibular cortex. Acta Otolaryngol (Stockh) Suppl 520:110–112

Talairach J, Tournoux P (1988) Co-planar stereotaxic atlas of the human brain. Three-dimensional proportional system: an approach to cerebral imaging. G. Thieme, New York

Teuber HL, Mishkin RG (1954) Judgment of visual and postural vertical after brain injury. J Psychol 38:161–175

Vitte E, Derosier C, Caritu Y, Berthoz A, Hasboun D, Soulié D (1996) Activation of hippocampal formation by vestibular stimulation. A functional magnetic imaging study. Exp Brain Res 112:523–526